Experimental Mechanics
https://doi.org/10.1007/s11340-024-01057-x

RESEARCH PAPER

Data-Driven Accelerated Parameter Identification for Chaboche-Type Visco-Plastic Material Models to Describe the Relaxation Behavior of Copper Alloys

L. Morand[1] · E. Norouzi[1,2] · M. Weber[1] · A. Butz[1] · D. Helm[1]

Received: 21 August 2023 / Accepted: 11 March 2024

Abstract

Background Calibrating material models to experimental measurements is crucial for realistic computational analysis of components. For complex material models, however, optimization-based identification procedures can become time-consuming, particularly if the optimization problem is ill-posed.

Objective The objective of this paper is to assess the feasibility of using machine learning to identify the parameters of a Chaboche-type material model that describes copper alloys. Specifically, we apply and analyze this identification approach using short-term uniaxial relaxation tests on a C19010 copper alloy.

Methods A genetic algorithm forms the basis for identifying the parameters of the Chaboche-type material model. The approach is accelerated by replacing the numerical simulation of the experimental setup by a neural network surrogate. The neural networks-based approach is compared against a classic approach using both, synthetic and experimental data.

Results The results show that on the one hand, a sufficiently accurate identification of the material model parameters can be achieved by a classic but time-consuming genetic algorithm. On the other hand, it is shown that machine learning enables a much more time-efficient identification procedure, however, suffering from the ill-posedness of the identification problem.

Conclusion Compared to classic parameter identification approaches, machine learning techniques can significantly accelerate the identification procedure for parameters of Chaboche-type material models with acceptable loss of accuracy.

Keywords Chaboche-type model · Copper alloy · Genetic algorithm · Ill-posed problem · Machine learning · Parameter identification · Neural networks · Relaxation test

Introduction

Motivation

Copper alloys play a central role in electronic components, which are increasingly demanded due to the ongoing digital transformation in industry and the upcoming transformation towards a green economy. Often, copper-based electric components (e.g. plug connectors) suffer harsh loading conditions, like cyclic and long-term thermo-mechanical loading. To analyze, design, and assess components in such environments, it is essential to take into account the time- and temperature-dependent behavior of copper alloys in component simulations. For this purpose, a visco-plastic material model of Chaboche-type can be used, as it is described, for example, in [1–3].

Calibrating the parameters of Chaboche-type material models to represent real material behavior is both, experimentally and computationally expensive. The present paper primarily focuses on the latter by analyzing the usage of machine learning methods. Specifically, neural networks are used to accelerate the identification procedure. In particular, the identification problem at hand is ill-posed in terms of the sensitivity of the parameters of the Perzyna term used in the Chaboche-type model. We will show that a perfect identification of the parameters of the Perzyna term is challenging and requires a highly accurate prediction model. For

✉ L. Morand
lukas.morand@iwm.fraunhofer.de

[1] Fraunhofer Institute for Mechanics of Materials IWM, Wöhlerstraße 11, Freiburg 79108, Germany

[2] FIZ Karlsruhe - Leibniz Institute for Information Infrastructure, Hermann-von-Helmholtz-Platz 1, 76344 Eggenstein-Leopoldshafen, Germany

Published online: 21 March 2024

evaluation, we use a large set of synthetic data as well as experimental data obtained from short-term uniaxial relaxation tests on a C19010 copper alloy.

Related Work

Identifying parameters that fit material model responses to experimental measurements is a common task in mechanical engineering and has been investigated widely in literature. Such parameter identification problems are typically approached by formulating an optimization problem. These optimization problems are inverse problems, which are often ill-posed and therefore challenging to solve. Typically, optimization problems are addressed by using optimization algorithms that explore the space of material model parameters to find suitable parameter combinations that match experimental observations [4]. Gradient-based optimization algorithms, for example, aim to minimize an objective function by using its gradient with respect to the material model parameters. This objective function represents a measure of the difference between experimental observations and the result of a simulated experiment. For an extensive overview of optimization methods, we refer to [5].

In complex identification problems, such as ill-posed and high-dimensional problems, the number of required function evaluations performed by gradient-based optimization algorithms and the quality of the solution depends strongly on the chosen starting points. Alternatively, gradient-free genetic algorithms can be used for complex identification problems. These algorithms aim to find a global solution by combining parameter vectors (so-called individuals) using operations, such as mutation, recombination and crossover (c.f. [6]). Yet, the number of function evaluations required by genetic algorithms is typically larger. Both, gradient-based optimization approaches and genetic algorithms, are fully deterministic, which means that only a limited number of solutions can be identified. To overcome this issue, Bayesian inference can be used to identify probability distributions for parameters fitting the material model to experimental measurements [7].

Regarding Chaboche-type material models, several parameter identification strategies have been developed and applied so far. Recently published approaches use Bayesian inference for identifying parameter distributions for given experimental measurements [8–10]. In [8], parameter distributions are identified at high-temperature cyclic loading tests of copper alloys. In [9], parameter distributions of a Chaboche-type material model including a damage formulation are identified at tensile and creep tests. In both works, [8, 9], it is pointed out that having knowledge about the prior parameter distribution is essential for identifying the posterior parameter distribution correctly. In addition, in [10], the authors compare several methods for updating probability distributions to estimate parameter values of a Chaboche-type material model with a damage formulation. The methods are evaluated using synthetic data obtained from one-element tests.

In contrast to Bayesian inference, the use of deterministic optimization approaches for identifying Chaboche-type material model parameters has been investigated since decades. In the present paper, we focus on such methods and therefore, in the following, we present approaches that have been described in literature so far. For example, in [11], gradient-based optimization algorithms and genetic algorithms are analyzed for fitting a visco-plastic material model to monotonic and cyclic loading tests. The results show that gradient-based optimization algorithms require fewer function evaluations than genetic algorithms. The starting points, however, need to be chosen appropriately. Particularly, the identification of the parameters of the recovery terms of Chaboche-type material models depend heavily on the defined starting points, as is shown in [12]. This indicates that the identification problem is ill-posed and emphasizes the need for a careful consideration of the optimization algorithm and starting points.

For such reasons, several publications provide heuristics for determining starting points for gradient-based optimization algorithms used to identifying parameters of Chaboche-type material models, see [13, 14]. Moreover, the approach published in [13] describes a staggered parameter identification scheme, in which subsets of the material model parameters are identified step-by-step on the basis of different experiments (cyclic, relaxation and creep tests). In contrast, in [14], all model parameters are identified in one step on the basis of cyclic tests. In terms of copper alloys, a step-by-step gradient-based optimization procedure was developed in [1] using low cycle fatigue and stress relaxation tests. Even an interactive tool for automatic parameter identification for visco-plastic material models has been developed and described in [15].

In contrast to the above described gradient-based approaches, genetic algorithms are often impractical since they typically need a larger number of function evaluations. To overcome this issue, machine learning can be applied in order to replace the numerical simulation by a faster data-driven surrogate model. In terms of parameter identification, surrogate modeling has widely been used for surrogate-based optimization (c.f. [16]). For example, in [17], surrogate-based optimization is used to identify elastic and plastic material model parameters on the basis of load-displacement curves measured in nano-indentation tests. In contrast, in the present publication, we aim to train a global surrogate to completely replace the numerical simulation in order to accelerate the optimization approach. This enables us to efficiently solve the parameter identification problem for measurements of different materials,

and thus, for variable objective functions. An example for such an approach is given in [18] for a complex materials design problem.

As an alternative to optimization-based approaches, also, the use of direct inverse models needs to be mentioned. In this approach, machine learning techniques are used to directly learn the inverse relation between the material model response and material model parameters [4]. This idea has been introduced originally in [19] at the example of identifying parameters of a Chaboche-type material model. Further, in [20, 21], for example, neural networks are used to identify parameters of a finite deformation plasticity model on the basis of spherical indentation tests. In [22], a neural network is used to identify parameters of an elasto-plastic material model for a composite material under cyclic loading. Also on the basis of cyclic loading tests, in [23], a neural network is used to identify parameters of a Chaboche-type material model for shape memory alloys. However, when inverse problems are ill-posed, neither state-of-the-art machine learning methods can be applied to learn inverse relations nor sampling can be done in a goal-directed manner, see [24] as well as [25, 26]. For these reasons, direct inverse models are not addressed in the present publication.

Contribution

When identifying the parameters of Chaboche-type material models, the success of parameter identification approaches using gradient-based optimization algorithms depends heavily on the starting points. This can be overcome by using computationally expensive genetic algorithm-based approaches. These can be made efficient with the use of machine learning-based surrogate models. In this regard, the present work analyzes

- the general ability of identifying parameters of a Chaboche-type material model using a genetic algorithm, with an emphasize on the ill-posedness of the inverse identification problem.
- the advantages and disadvantages of accelerating the parameter identification procedure using neural networks by comparing the approach to a classic approach that does not rely on machine learning.
- the general capability for parameters of Chaboche-type material models to be identified correctly.

We would like to emphasize that for short-term uniaxial relaxation tests, accelerating the identification procedure is typically not necessary, as classic approaches already perform well. However, when dealing with long-term relaxation tests or experiments with a more complex geometry that have to be modeled using for example the Finite Element Method, the acceleration of parameter identification approaches becomes inevitable. Therefore, the present paper aims to study the parameter identification problem for Chaboche-type material models and the application of a surrogate model at the example of short-term uniaxial relaxation tests. It should be noted that the challenges in parameter identification remain similar regardless of the specific type of experiment conducted.

Methods

Parameter Identification Strategies

The basis for identifying material model parameters are experimental measurements that show significant characteristics of the material behavior and a numerical simulation of the conducted experiment (c.f. Fig. 1). The output of the numerical simulation, denoted as $\boldsymbol{C} \in \mathbb{R}^k$, needs to correspond to the discretized experimentally measured material response, denoted as $\boldsymbol{C}^{\text{exp}} \in \mathbb{R}^k$, for a given set of material model parameters, denoted as $\boldsymbol{p} \in \mathbb{R}^l$. Here, k refers to the number of discrete measurements and l refers to the number of material model parameters. $\boldsymbol{C}$ and $\boldsymbol{p}$ are related using the numerical simulation, represented as an operator g in the following:

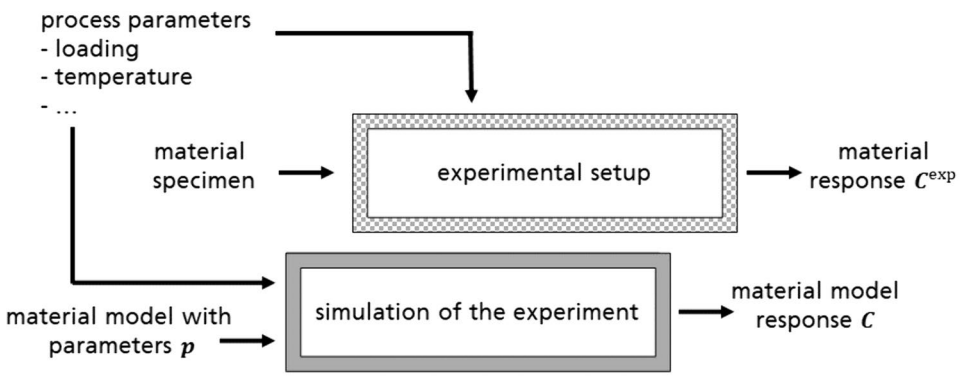

Fig. 1 Comparison between experiment and numerical simulation including the relevant input and output parameters

$$\boldsymbol{C} = g(\boldsymbol{p}). \tag{1}$$

To identify optimal material model parameters $\boldsymbol{p}^*$ for given measurements $\boldsymbol{C}^{\text{exp}}$, optimization methods minimize a distance measure between the experimental measurement and the calculated response. The distance measure can be defined for example by the root mean squared error:

$$\boldsymbol{p}^* = \arg\min_{\boldsymbol{p}} \sqrt{\frac{1}{k}\sum_{i=1}^{k}(C_i^{\text{exp}} - C_i)^2}. \tag{2}$$

In this case, the values of C_i^{exp} and C_i are weighted equally. In the following, we refer to this approach (incorporating the numerical simulation g directly) as classic optimization approach.

Alternatively, machine learning models can be used to replace the time-consuming numerical simulation in the classic optimization approach. For this accelerated optimization approach, a machine learning surrogate $\tilde{g}$ is trained aiming to replace g in equation (1):

$$\boldsymbol{C}^{\text{ML}} = \tilde{g}(\boldsymbol{p}, \boldsymbol{\theta}), \tag{3}$$

where $\boldsymbol{C}^{\text{ML}} \in \mathbb{R}^k$ denotes the predicted simulation response, and $\boldsymbol{\theta}$ denotes the trainable parameters of the machine learning model. Consequently, in equation (2) C_i is replaced by C_i^{ML}.

By replacing g with its machine learning surrogate $\tilde{g}$, the classic optimization strategy is accelerated, as the learned model typically executes faster than the numerical simulation. This advantage grows with the complexity and, accordingly, the duration of the numerical simulation. However, it is important to note that the surrogate model is not as accurate as its simulation counterpart, and, therefore, its use comes with the cost of numerical accuracy. Illustrations of the accelerated optimization approach and the classic optimization approach are depicted in Fig. 2.

To solve the identification problem (equation (2)), in this study, we use the genetic algorithm *Differential Evolution* [27] as it is implemented in Python package *SciPy* [28]. *Differential Evolution* aims to find a global minimum by, in this implementation, consecutively performing the operations mutation, crossover and selection, see [29] for details.

Visco-Plastic Material Model for Copper Alloys

In the following, we describe the used visco-plastic material model for copper alloys in its one-dimensional form based on the description in [2]. Particularly, the model is a modified plasticity model that accounts for the rate-dependent behavior using a Perzyna multiplier. It also includes a yield-function of von Mises-type as well as isotropic and kinematic hardening. Consequently, it can be classified as a Chaboche-type model.

In the elastic regime, the linear stress-strain relation is defined by the Young's modulus:

$$\sigma = E\varepsilon_{\text{el}}. \tag{4}$$

The elastic strain ε_{el} is derived from $\varepsilon = \varepsilon_{\text{el}} + \varepsilon_{\text{p}}$, with the plastic strain ε_{p}. The yield function, which describes the onset of plastic deformation, is given as

$$f = \sigma_{\text{eq}} - \sigma_{\text{y}} \leq 0, \tag{5}$$

where σ_{eq} denotes the von-Mises equivalent stress and σ_{y} the actual yield stress. The yield stress is defined by an isotropic hardening model:

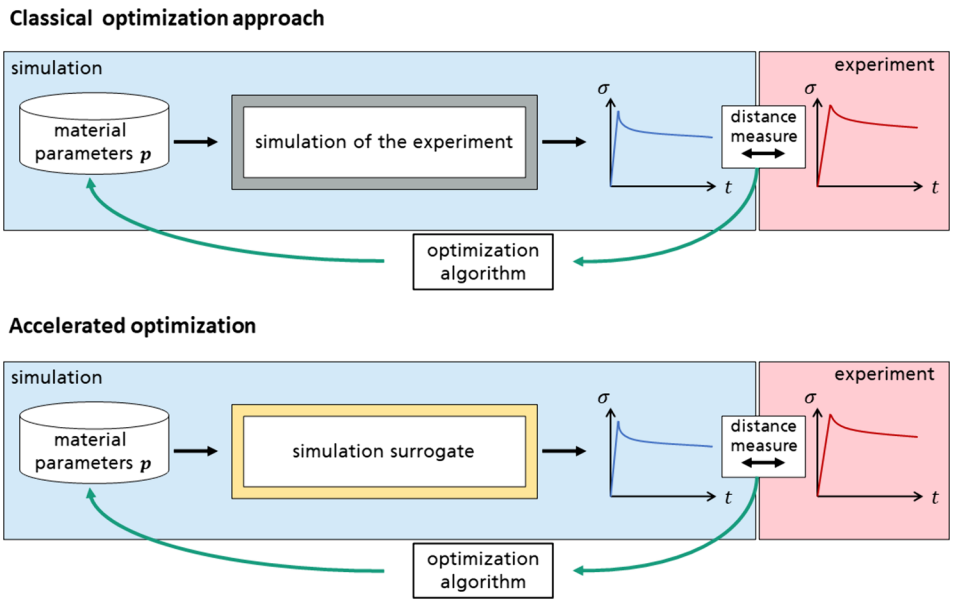

Fig. 2 The classic optimization approach minimizes a distance measure between the experimentally measured material response and the simulated one (top). In the accelerated optimization approach, the numerical simulation is replaced with a machine learning surrogate (bottom). In its basic form, this figure originates from [30]

$$\sigma_y = R_0 + R, \tag{6}$$

in which R_0 is the initial yield stress and R describes the hardening behavior [31]. R is defined by

$$R = \sum_i R_i. \tag{7}$$

The individual terms R_i can be calculated by

$$\dot{R}_i(\dot{\varepsilon}_p, R_i) = \gamma_i \dot{\varepsilon}_p - (\beta_i \dot{\varepsilon}_p + \alpha_i) R_i, \tag{8}$$

in which $\dot{\varepsilon}_p$ is the plastic strain rate and β_i, γ_i, α_i are material dependent parameters. While the parameters β_i and γ_i are mostly responsible for the hardening behavior, the parameter α_i is part of the recovery term and affects the long-term plastic behavior of the material [32].

In this study, the number of hardening terms is set to $i = 2$ in order to describe the hardening behavior of rolled copper sheets [3]. These typically show a nonlinear hardening behavior at comparably low plastic strain and a slowly increasing linear hardening behavior for higher plastic strains. To describe this behavior, we set the parameters of the second hardening term to $\beta_2 = 1$ MPa and $\alpha_2 = 0$.

The influence of the strain rate on the yield stress is applied with the approach according to Perzyna [33]:

$$\dot{\varepsilon}_p = \frac{1}{\eta} \left\langle \frac{f}{r} \right\rangle^m, \tag{9}$$

where η is the temperature dependent viscosity and m the rate sensitivity exponent. The parameter r is a constant, which is set to 1 MPa in order to ensure that f/r remains dimensionless. The angular brackets in equation (9) represent the Macaulay brackets (i.e. $\langle x \rangle = \frac{|x|+x}{2}$).

On the whole, the material model contains eight material dependent parameters, which are E, R_0, η, m, α_1, β_1, γ_1, and γ_2. The main effect of these parameters on the material behavior is illustrated in Fig. 3 at the example of a stress-time curve typically originating from uniaxial relaxation tests. The temperature dependence of copper material can be controlled indirectly by varying the above mentioned parameters. Investigations in literature assume that the influence of temperature on the variation of the material model parameters follows approximately a linear relation, see [3, 34].

Simulating Uniaxial Relaxation Tests

Within this study, short-term uniaxial relaxation tests were conducted to measure characteristics of the material response of C19010 copper alloy. The relaxation tests under consideration consist of a loading step followed by a holding period at a fixed temperature. During loading, a strain rate of $\dot{\varepsilon} = 0.001\ \mathrm{s}^{-1}$ is applied for 20 seconds to apply a total strain of 2%. After that, a holding step is applied for 7100 seconds. Figure 4 depicts experimentally measured stress-strain curves and the corresponding stress-time curves that follow from these conditions.

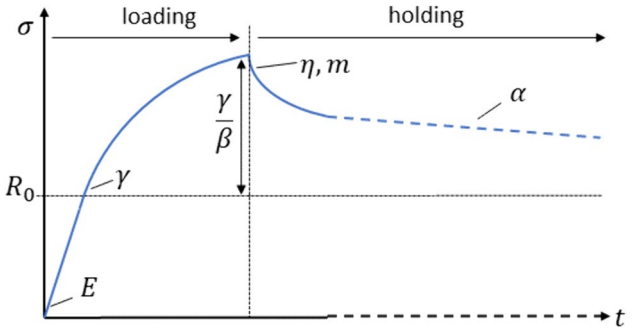

Fig. 3 Main effect of the parameters on the material model behavior at the example of a stress-time curve typically originating from uniaxial relaxation tests. The figure originates from [30]

For the purpose of this work, a numerical simulation of the above described experiment was set up. To get the one-dimensional time-dependent stress response, we solve the initial value problem described by equations (4) to (9) numerically using the LSODA solver implemented in Python package *scipy.integrate* [28]. LSODA uses a combination of Adams-Moulton methods and backward differentiation formulas with an automatic switching approach, as it is described in detail in [35, 36]. Using the numerical simulation, we calculate stress values at defined time points τ_i resulting in a discretized stress-time curve $\sigma(\tau_i)$ for a given set of material model parameters $\boldsymbol{p}$:

$$\sigma(\tau_i) = g(\boldsymbol{p}). \tag{10}$$

The time discretization τ_i for the LSODA solver is chosen to be fine when plastic deformation starts until the beginning of the holding period and coarser in the elastic regime and during holding. In total, time is discretized via 300 integration points, of which 150 are located in the loading and 150 in the holding period.

In order to fit the simulation response to the obtained measurements, optimal material model parameters

$$\boldsymbol{p}^* = (E^*, R_0^*, \eta^*, m^*, \alpha_1^*, \beta_1^*, \gamma_1^*, \gamma_2^*) \tag{11}$$

need to be identified. Alternatively, the parameters E and R_0 can be identified in beforehand on the basis of quasi-static tension tests. However, the identification of the yield strength R_0 can turn out to be challenging for this type of material, as there is typically no sharp transition point between elastic and plastic behavior.

The parameter ranges inside which we operate are described in Table 1. Note that instead of limiting the range for γ_1, we limit the range of $\frac{\gamma_1}{\beta_1}$ as this relation defines

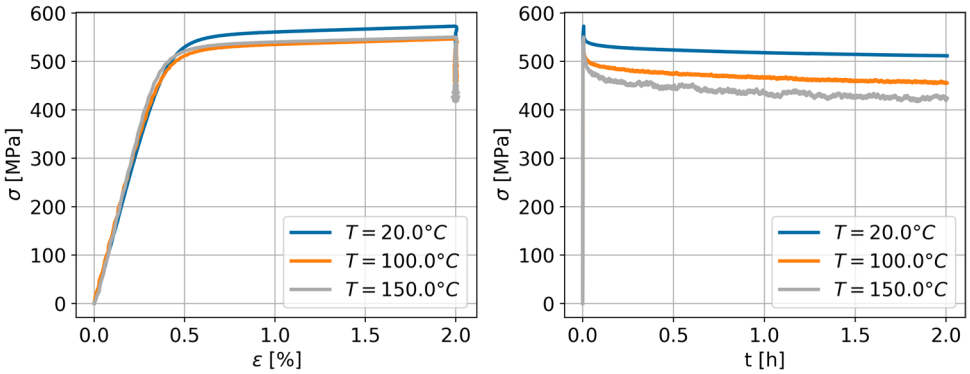

Fig. 4 Experimentally measured stress-strain curves (left) and corresponding stress-time curves (right) obtained from the conducted uniaxial relaxation tests of C19010 copper alloy at 20, 100 and 150 °C. The data originates from [30]

the value at which the hardening terms saturate, see [25]. A test set of 10000 data points (including material model parameters $\boldsymbol{p}$ and corresponding simulated stress-time curves $\sigma(\tau_i)$ is generated using random parameter variations within the defined parameter range. For training the neural network model, an additional set of one million data points is generated based on random parameter variations. This large amount of training data was generated to ensure that the trained model is not affected by a lack of data.

To evaluate the deviation between the fitted curve and the experimentally measured curve, we define the mean relative error ΔC between the target curve $\sigma^{\exp}(\tau_i)$ and the curve which is reconstructed using the identified parameters $\sigma(\tau_i) = g(\boldsymbol{p}^*)$. We define the mean relative error as being the mean absolute error

$$\Delta C_{\text{abs}} = \frac{1}{t_1 - t_0} \int_{t_0}^{t_1} |\sigma^{\exp}(t) - \sigma(t)| \, \mathrm{d}t \tag{12}$$

normalized by the maximum stress value occurring at the end of the loading phase:

$$\Delta C = \frac{\Delta C_{\text{abs}}}{\max(\sigma^{\exp}(t))}. \tag{13}$$

Table 1 Parameter ranges adopted from [37] and adjusted for the purpose of this study

parameter	min	max	unit
E	100	140	GPa
R_0	80	320	MPa
η	10^{50}	10^{75}	s
m	25	65	-
α_1	10^{-6}	10^{-3}	s^{-1}
β_1	500	3000	-
γ_1/β_1	50	220	MPa
γ_2	500	2500	MPa

Results

Identifying Parameters Using the Classic Optimization Approach

Due to limited computation resources, we used only 100 test data points to validate the classic optimization-based parameter identification approach (corresponding to 100 optimization runs conducted). For the *Differential Evolution* algorithm, a population size of 60 was chosen with a recombination factor of 0.7, and a mutation factor randomly drawn from a uniform distribution between 0.0 and 1.0 in every iteration. The objective function was defined based on the root mean squared error (c.f. equation (2)). In total, the *Differential Evolution* algorithm performed 1200 iterations per optimization run, for the purpose of this study. This number has shown to be adequate to identify the material model parameters correctly in most of the runs.

The results for identifying parameters using the above described settings are depicted in Fig. 5, presented as parity plots (true vs. identified material model parameters). The identified parameters (except for η and m) are almost exactly on the identity line, which means that the parameters are identified correctly. The parameters η and m, in contrast, do not always lie on the identity line indicating that the algorithm was not able to identify them correctly in all the cases. Nevertheless, the mean relative errors ΔC are close to zero, as can be seen in the histogram in Fig. 6. Even the worst ΔC values are remarkably small.

Surrogate Model Training

In order to replace the numerical simulation that was used in the previous section, we trained a surrogate model on the corresponding inputs and outputs. The purpose of the surrogate model is to predict the discretized stress-time curve for a given set of material model parameters:

$$\hat{\sigma}(\tau_i) = \tilde{g}(\boldsymbol{p}, \boldsymbol{\theta}). \tag{14}$$

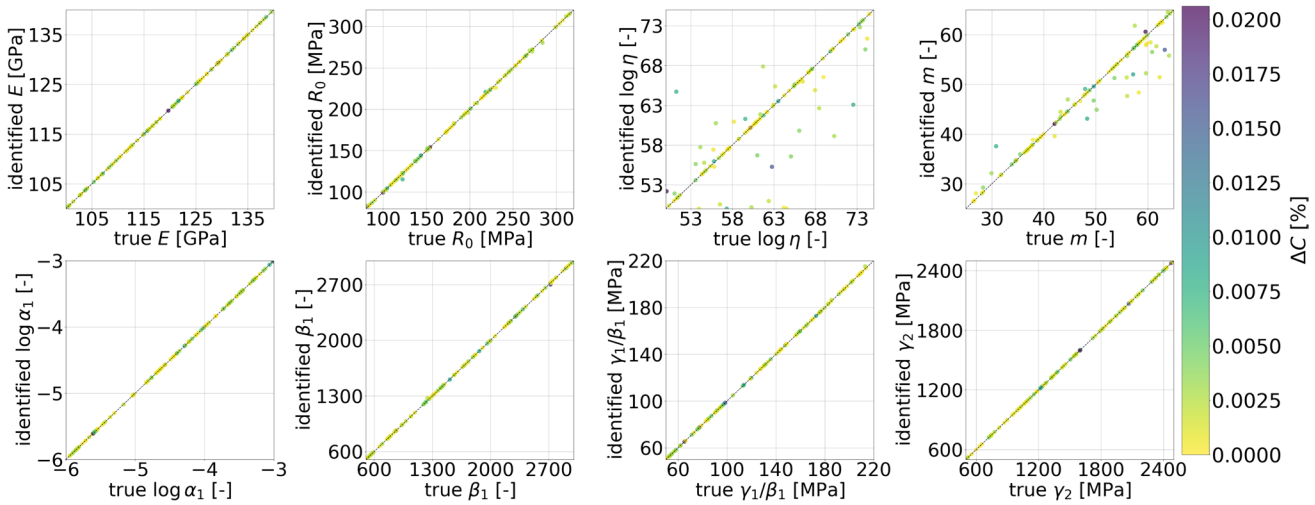

Fig. 5 Parity plots for parameters identified by the *Differential Evolution* algorithm incorporating the numerical simulation. The mean relative error ΔC is color coded

To adjust the trainable parameters $\boldsymbol{\theta}$, the surrogate model is trained on the set of one million samples. Specifically, we use a feed forward neural network to learn the mapping (see [38] for a general introduction).

The neural network model was trained by minimizing the mean squared error loss function using *ADAM* optimizer [39]. To avoid overfitting, L2 regularization [40] and early stopping [41] were applied. For the mapping to learn, a neural network with two hidden layers turned out to be adequate. The architecture of the trained neural network is illustrated in Fig. 7. The neural network used ReLU activation functions. The hyperparameters of the neural network (i.e., number of neurons in the hidden layers and the L2 regularization parameter) were optimized using Bayesian hyperparameter optimization on the basis of Gaussian processes [42]. We used the Python package *scikit-optimize* [43] for this purpose.

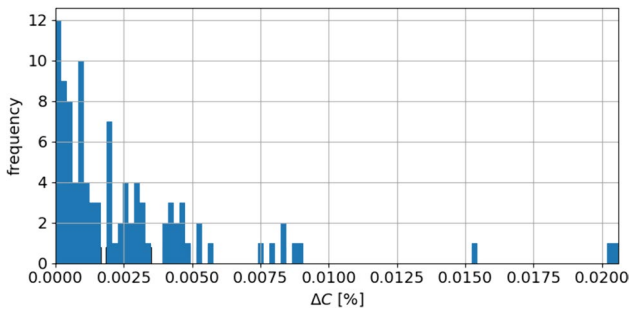

Fig. 6 Histogram showing the mean relative errors ΔC after identifying parameters using the *Differential Evolution* algorithm incorporating the numerical simulation ΔC

Beforehand, we studied the prediction quality of the neural network models in relation to the number of training samples. To do so, we optimized the hyperparameters and trained several models on random subsets of the original data base. We use the mean relative error ΔC in the test set as performance measure. In particular, we trained ten models on different random subsets for a predefined sample number and evaluated their performance. Figure 8 shows the average mean relative error of the models as well as the individual errors for each of the trained models. For the full training set, only one model was trained.

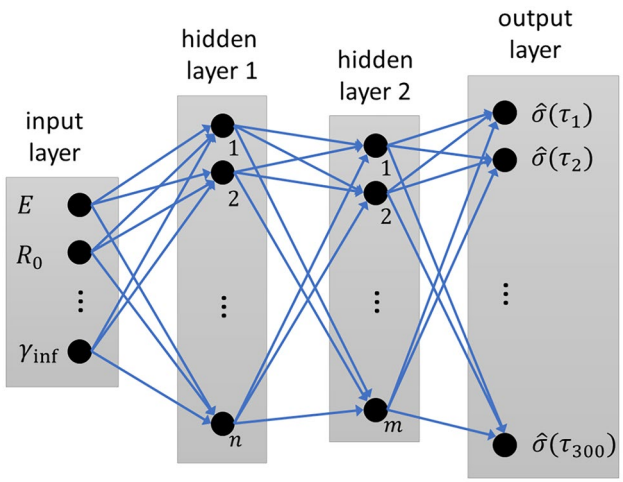

Fig. 7 Architecture of the trained feed forward neural networks with two hidden layers containing n and m neurons, respectively. The inputs of the neural network are the material model parameters $\boldsymbol{p}$, and the outputs are the discretized stress-time curve $\hat{\sigma}(\tau_i)$

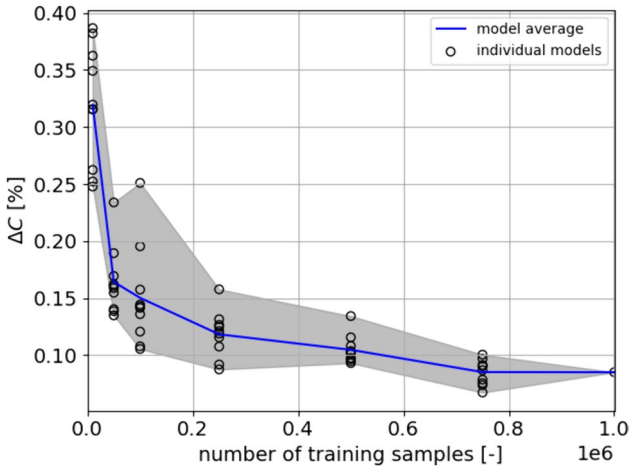

Fig. 8 Performance of neural network models trained on different datasets: Range of reached mean absolute errors ΔC vs. number of samples in the training sets

As was to be expected, the prediction quality increases with the number of training samples. Also, the fluctuation of prediction quality withing the models trained with the same number of samples decreases. Some exceptions can be observed, which can be due to the random choice of samples in the training set. The mean relative error ΔC in the test set, however, converges only slowly with a growing number of samples. It is therefore hard to get the model as accurate as the numerical simulation. The neural network model used for the accelerated optimization was the one trained on the full dataset. The neural network consisted of two hidden layers with 241 and 87 neurons, respectively. For L2 regularization a regularization parameter of $\lambda = 1.01\text{e}^{-5}$ was applied.

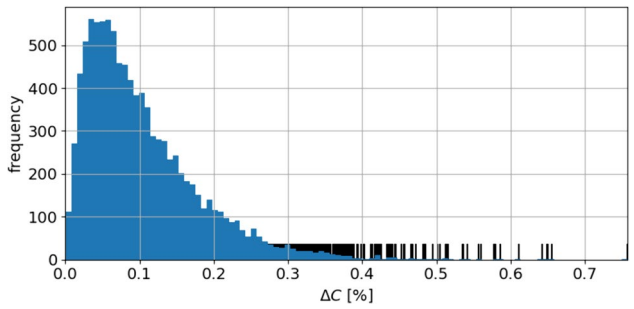

Fig. 10 Histogram showing the mean relative errors ΔC after identifying parameters using the *Differential Evolution* algorithm incorporating the surrogate model. The black lines mark ΔC of individual samples

Identifying Parameters Using the Accelerated Optimization Approach

To facilitate comparison with the results from the classic optimization approach, we used the same setting for the *Differential Evolution* algorithm in the accelerated optimization approach. 1200 iterations were performed with a population size of 60, optimizing the root mean squared error (c.f. equation (2)).

The results obtained are depicted in Fig. 9 as parity plots. Similar to the results from the classic optimization approach, the figure shows that all parameters can be identified almost correctly except for η and m. Although, the parameters η and m cannot be identified correctly, the mean relative errors ΔC are relatively low. This can also be seen in the histogram depicted in Fig. 10 showing the mean relative errors ΔC in the test set. The mean relative errors ΔC, however,

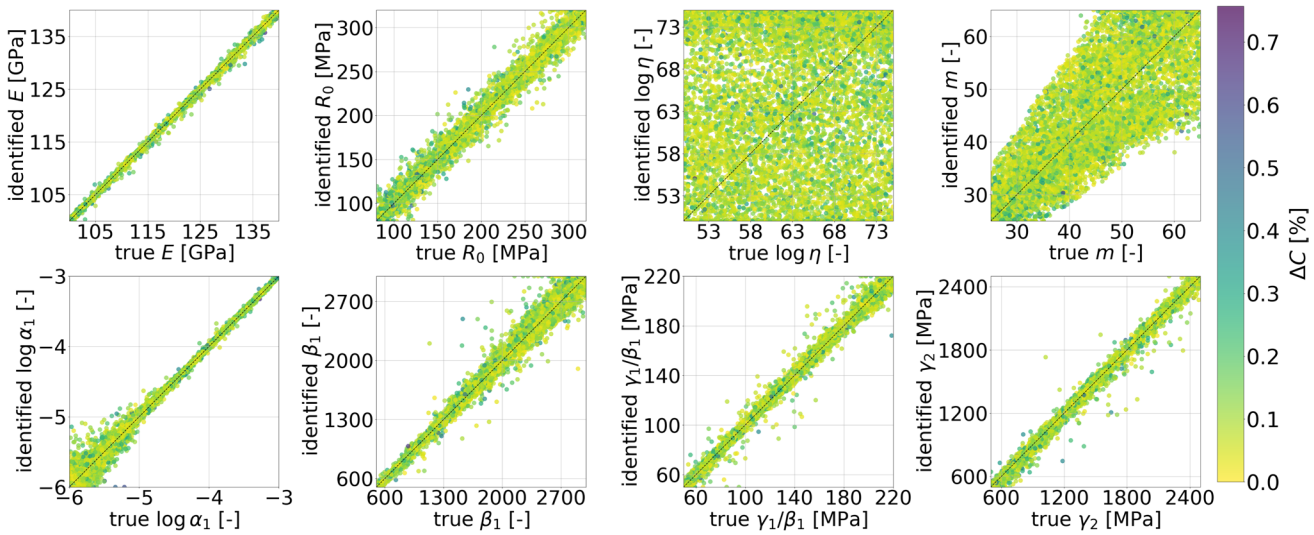

Fig. 9 Parity plots for parameters identified by the *Differential Evolution* algorithm incorporating the surrogate model. The mean relative error ΔC is color coded

Table 2 Parameters identified by the classical optimization approach and the corresponding errors ΔC_{abs} and ΔC

T [°C]	E [GPa]	R_0 [MPa]	η [s]	m [-]	α_1 [s^{-1}]	β_1 [-]	$\frac{\gamma_1}{\beta_1}$ [MPa]	γ_2 [MPa]	ΔC_{abs} [MPa]	ΔC [%]
20	126.7	287.3	1e75.0	32.4	1e-4.6	1664.7	98.5	1393.5	0.4	0.1
100	133.2	192.6	1e75.0	30.5	1e-4.3	1725.3	103.9	1432.7	1.0	0.2
150	135.7	117.1	1e75.0	28.5	1e-4.0	1758.9	82.6	1559.3	4.2	0.8

are one magnitude higher compared to the ones from the classic parameter identification approach. In contrast, on average, the execution speed was about 5.1 times higher (by using only one CPU) compared to the classic approach (by using 28 of the same CPUs). However, we have to remark here that this can only be understood as a rough estimate, as we did not optimize and benchmark the execution speed systematically.

Application to Experimental Data

As a further study, we apply the accelerated optimization approach to identify parameters on the basis of experimentally measured short-time relaxation curves of C19010 copper-alloy specimens. For this purpose, tests at three different temperatures ($T = 20$°C, $T = 100$°C and $T = 150$°C) have been conducted with the conditions described in the "Simulating Uniaxial Relaxation Tests" section. For comparison, we additionally applied the classic optimization approach. The parameters identified by the classic optimization approach are listed in Table 2, the ones identified by accelerated optimization are listed in Table 3. The corresponding mean absolute and relative errors, ΔC_{abs} and ΔC, are also shown in both tables.

A closer look at Tables 2 and 3 reveals that both approaches yield similar parameters. The identified parameters η, m and α_1 are identical for 100°C and 150°C. For 20°C, m and α_1 are identical. The identified values for the Young's modulus are identical across all temperatures except for small differences in the decimal places. All other identified parameters are similar to one other. For this reason, the mean absolute and relative errors, C^{abs} and ΔC, are similarly low from an engineering point of view. The slightly higher errors obtained when fitting the curve at $T = 150$°C is caused by measurement inaccuracies that occured at the beginning and at the end of the holding period. These inaccuracies can be seen clearly in Fig. 11, which shows the measured relaxation curves together with the curves reconstructed from the parameters identified by the accelerated optimization approach.

Finally, we want to remark that the values identified for model parameter η all lie at the upper bound of the defined parameter space. While it is possible that the true values lie above this bound, we did not observe significant changes in the material behavior with increasing η values (which is mainly compensated by increasing m values). Furthermore, since the identification approaches already yield sufficiently accurate results, the parameter space was not adjusted in this study.

Discussion

The results from the classic optimization approach show that the global optimizer *Differential Evolution* is able to identify parameters of the Chaboche-type material model for copper alloys. This can be seen in Fig. 5, as the true and identified parameters match for the majority of the test samples. Even if parameters are not identified correctly, the mean relative errors ΔC are remarkably small, what indicates the presence of a sensitivity problem. It is to be expected, however, that given a sufficiently large population size and enough run time, the parameters for all of the test samples can be identified correctly. In this study, even by using 28 CPUs per run, only 100 of the 10000 test samples could be used for evaluating the classic optimization approach due to limited time resources.

In contrast, the accelerated optimization approach allowed us to evaluate all 10000 test data points in an adequate period of time using only one CPU per run. The accelerated optimization approach was able to identify the material model parameters, resulting in small deviations between the true and reconstructed curves ($\Delta C < 1\%$). These results are considered to be sufficiently accurate from an engineering point of view. Moreover, most of the parameters (E, R_0, α_1, β_1, $\frac{\gamma_1}{\beta_1}$ and γ_2) were identified correctly, see Fig. 9. In addition, Fig. 9 reveals that particularly the identification of the parameters η and m is

Table 3 Parameters identified by the accelerated optimization approach and the corresponding errors ΔC_{abs} and ΔC

T [°C]	E [GPa]	R_0 [MPa]	η [s]	m [-]	α_1 [s^{-1}]	β_1 [-]	$\frac{\gamma_1}{\beta_1}$ [MPa]	γ_2 [MPa]	ΔC_{abs} [MPa]	ΔC [%]
20	126.7	314.6	1e64.2	28.2	1e-4.6	1427.5	91.4	1304.9	0.4	0.1
100	133.2	184.5	1e75.0	30.5	1e-4.3	1895.6	109.0	1502.6	0.9	0.2
150	135.9	106.6	1e75.0	28.5	1e-4.0	1976.7	89.6	1565.4	4.1	0.7

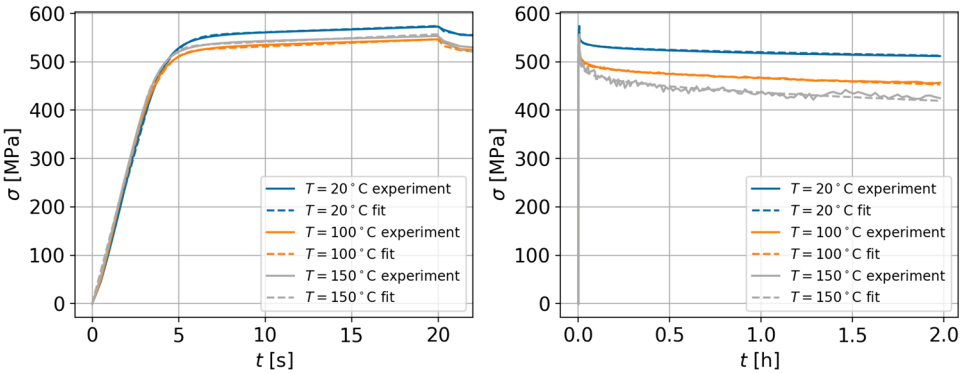

Fig. 11 Experimentally measured short-time relaxation curves at different temperatures and curves fitted by the accelerated optimization approach. The left plot zooms in the loading phase, while the right plot shows the complete measurement

challenging and the optimization strategy gets stuck in local optima. This is, however, not only due to the ill-posedness of the identification problem, but also due to the inherent inaccuracy of the neural network predictions compared to the numeric solution. These deviations, along with the sensitivity problem, pose a challenge for the accelerated optimization approach to uniquely identify the material model parameters η and m. In this study, this problem is intensified for parameter sets containing large m values and is, therefore, also depending on the defined parameter space.

Nevertheless, when applying the accelerated optimization approach to experimental data, the sensitivity problem has only a minor effect due to measurement inaccuracies. In addition, it is not possible to investigate this issue fundamentally, because the true parameters are unknown and we have to rely solely on the error measure ΔC. Thus, we analyzed only the similarity between the parameters identified by the classic and the accelerated optimization approach. By doing so, it can be seen that both approaches are equally effective for identifying the material model parameters for the given experimental curves, as the identified parameters are similar to each other. Moreover, trends can be observed for the identified parameters such as an increasing Young's modulus and a decreasing initial yield stress with increasing temperature. All of the parameters identified by the accelerated optimization approach exhibit similar trends, except for $\frac{\gamma_1}{\beta_1}$ (however, the identified values for $\frac{\gamma_1}{\beta_1}$ are quite close to each other). As the latter is the case for both, the classic and the accelerated optimization approach, we assume that this is due to measurement inaccuracies. Furthermore, we do not expect the Young's modulus to vary significantly within the applied temperature range, which is why we trace this observation back to measurement inaccuracies, also.

In addition, as can be seen in Fig. 11, both approaches are robust against experimental noise, in contrast to direct inverse modeling approaches (c.f. [25]). Compared to the classic optimization approach, the accelerated optimization approach is much faster and thereby allows for a broad scale search for optimal material model parameters in an adequate period of time.

Summary and Outlook

The results of the present study demonstrate that a nearly perfect fit of parameters of Chaboche-type material models to short-term uniaxial relaxation tests can be achieved by using genetic algorithms. Although only a one-dimensional model formulation was considered, genetic algorithms in combination with numerical solvers requires significant computation time. In contrast, parameter identification approaches can be applied efficiently when replacing the numerical simulation of the experiment with a fast machine learning surrogate. Using feed forward neural networks, for example, the identification procedure can be accelerated with acceptable loss of accuracy from an engineering point of view. However, it is shown that even if the response of the Chaboche-type material model can be fitted accurately, the parameters of the used Perzyna approach cannot be identified uniquely using the neural network model presented in this study. To address this type of uncertainty, the application of Bayesian inference could be investigated in future work.

Indeed, it is important for material models used in industry to meet the long-term relaxation behavior, which is not captured in the short-time relaxation tests conducted within this study. However, long-term relaxation tests usually involve more elaborate test setups, such as cantilever tests, which require complex modeling techniques, such as Finite Element simulation models, to identify material model parameters. Therefore, it is crucial to assess the applicability of parameter identification strategies for Chaboche-type material models in simpler use cases beforehand, what was the aim of the present study.

Acknowledgements In the scope of the Programme for Industrial Collective Research (Industrielle Gemeinschaftsforschung, IGF), this project (number 21114 N) was funded by the German Federal Ministry for Economic Affairs and Climate Action via the German Federation of Industrial Research Associations - AiF (Arbeitsgemeinschaft industrieller Forschungsvereinigungen e.V.) based on a decision of the German Bundestag. In addition, we thank Miriam Eisenbart, Karin Pfeffer, Felix Bauer, Benjamin Schlay, and Ulrich Klotz from Forschungsinstitut Edelmetalle + Metallchemie at Schwäbisch Gmünd, Germany, for providing a sample set of experimental data.

Funding Open Access funding enabled and organized by Projekt DEAL.

Data Availability The data used in this study is available in the Zenodo repository at https://doi.org/10.5281/zenodo.10796926 [44].

Declarations

Competing Interests The authors have no competing interests to declare that are relevant to the content of this article.

References

1. Bouajila W, Riccius J (2016) Modelling of the cyclic and viscoplastic behavior of a copper-base alloy using Chaboche model. In: Space Propulsion, p 1–7
2. Weber M, Helm D (2018) Prediction of the behaviour of copper alloy components under complex loadings by electro-thermomechanical coupled simulations. Mater Sci Technol 36(8):899–905
3. Eisenbart M, Weber M, Pfeffer K, Dirk H, Klotz U (2018) Standardisierung der mechanischen Charakterisierung und Quantifizierung von Materialkennwerten zur Modellierung des zeitabhängigen Verformungsverhaltens von Halbzeugen aus hochleitfähigen Cu-Legierungen. Forschungsinstitut für Edelmetalle und Metallchemie, Schwäbisch Gmünd, Germany; Fraunhofer Institut für Weckstoffmechanik IWM, Freiburg, Germany. Report from IGF project 18597 N of the AiF Forschungsnetzwerk Mittelstand
4. Mahnken R (2004) Identification of material parameters for constitutive equations. Encyclopedia Comput Mech 2
5. Nocedal J, Wright SJ (2006) Numerical optimization, 2nd edn. Springer Science+Business Media, LLC
6. Beyer HG, Schwefel HP (2002) Evolution strategies - a comprehensive introduction. Nat Comput 1(1):3–52
7. Rappel H, Beex LA, Hale JS, Noels L, Bordas S (2020) A tutorial on Bayesian inference to identify material parameters in solid mechanics. Arch Comput Methods Eng 27(2):361–385
8. Janouchová E, Kučerová A (2018) Bayesian inference of heterogeneous viscoplastic material parameters. Acta Polytech CTU Proc 15:41–45
9. Chakraborty A, Messner M (2021) Bayesian analysis for estimating statistical parameter distributions of elasto-viscoplastic material models. Probab Eng Mech 66:103153
10. Adeli E, Rosić B, Matthies HG, Reinstädler S, Dinkler D (2020) Comparison of Bayesian methods on parameter identification for a viscoplastic model with damage. MDPI Metals 10(7):876
11. Mahnken R, Stein E (1996) Parameter identification for viscoplastic models based on analytical derivatives of a least-squares functional and stability investigations. Int J Plast 12(4):451–479
12. Schwertel J, Schinke B (1996) Automated Evaluation of Material Parameters of Viscoplastic Constitutive Equations. J Eng Mater Technol 118(3):273–280
13. Tong J, Zhan ZL, Vermeulen B (2004) Modelling of cyclic plasticity and viscoplasticity of a nickel-based alloy using Chaboche constitutive equations. Int J Fatigue 26(8):829–837
14. Gong Y, Hyde CJ, Sun W, Hyde T (2010) Determination of material properties in the Chaboche unified viscoplasticity model. Proc Inst Mech Eng Part L J Mater Des Appl 224(1):19–29
15. Saleeb A, Marks J, Wilt T, Arnold S (2004) Interactive software for material parameter characterization of advanced engineering constitutive models. Adv Eng Softw 35(6):383–398
16. Forrester AI, Keane AJ (2009) Recent advances in surrogate-based optimization. Prog Aerosp Sci 45(1–3):50–79
17. Li H, Gutierrez L, Toda H, Kuwazuru O, Liu W, Hangai Y et al (2016) Identification of material properties using nanoindentation and surrogate modeling. Int J Solids Struct 81:151–159
18. Iraki T, Morand L, Dornheim J, Helm D, Link N (2022) A multi-task learning-based optimization approach for finding diverse sets of microstructures with desired properties. Int J Intell Manuf
19. Yagawa G, Okuda H (1996) Neural networks in computational mechanics. Arch Comput Methods Eng 3(4):435–512
20. Huber N, Tsakmakis C (1999) Determination of constitutive properties fromspherical indentation data using neural networks. Part I: The case of pure kinematic hardening in plasticity laws. J Mech Phys Solids 47(7):1569–1588
21. Huber N, Tsakmakis C (1999) Determination of constitutive properties fromspherical indentation data using neural networks. Part II: Plasticity with nonlinear isotropic and kinematic hardening. J Mech Phys Solids 47(7):1589–1607
22. Lefik M, Schrefler B (2002) Artificial neural network for parameter identifications for an elasto-plastic model of superconducting cable under cyclic loading. Comput Struct 80(22):1699–1713
23. Helm D (2005) Pseudoelastic behavior of shape memory alloys: constitutive theory and identification of the material parameters using neural networks. Tech Mech 25(1):39
24. Jordan MI, Rumelhart DE (1992) Forward models: supervised learning with a distal teacher. Cogn Sci 16(3):307–354
25. Morand L, Helm D (2019) A mixture of experts approach to handle ambiguities in parameter identification problems in material modeling. Comput Mater Sci 167:85–91
26. Morand L, Link N, Iraki T, Dornheim J, Helm D (2022) Efficient microstructure property space exploration via active learning. Front Mater 8
27. Storn R, Price K (1997) Differential evolution - a simple and efficient heuristic for global optimization over continuous spaces. J Glob Optim 11(4):341–359
28. Virtanen P, Gommers R, Oliphant TE, Haberland M, Reddy T, Cournapeau D et al (2020) SciPy 1.0: Fundamental Algorithms for Scientific Computing in Python. Nature Methods 17:261–272
29. Herrera F, Lozano M, Verdegay JL (1998) Tackling real-coded genetic algorithms: operators and tools for behavioural analysis. Artif Intell Rev 12:265–319
30. Morand L, Weber M, Butz A, Dirk H, Eisenbart M, Pfeffer K et al (2023) Qualifizierung von standardisierten Langzeitversuchen an Kupferwerkstoffen zur wirtschaftlichen Bestimmung von Materialparametern für CAE-Anwendungen. Forschungsinstitut für Edelmetalle und Metallchemie, Schwäbisch Gmünd, Germany; Fraunhofer Institut für Weckstoffmechanik IWM, Freiburg, Germany. Report from IGF project 21114 N of the AiF Forschungsnetzwerk Mittelstand
31. Helm D (2006) Stress computation in finite thermoviscoplasticity. Int J Plast 22(9):1699–1727
32. Chaboche JL (2008) A review of some plasticity and viscoplasticity constitutive theories. Int J Plast 24(10):1642–1693
33. Perzyna P (1963) The constitutive equations for rate sensitive plastic materials. Q Appl Math 20(4):321–332

34. Uppaluri R, Helm D (2016) Thermomechanical characterization of 22MnB5 steels with special emphasis on stress relaxation and creep behavior. Mater Sci Eng A 658:301–308
35. Hindmarsh AC (1983) ODEPACK, a systematized collection of ODE solvers. IMACS Trans Sci Comput 1:55–64
36. Petzold L (1983) Automatic selection of methods for solving stiff and nonstiff systems of ordinary differential equations. SIAM J Sci Stat Comput 4(1):136–148
37. Norouzi E (2020) Analysis and application of machine learning approaches to identify parameters of a visco-plastic material model based on numerical and experimental data of copper. ICAMS, Ruhr-Universtität Bochum; completed at Fraunhofer IWM Freiburg. Master's Thesis
38. Haykin S (1999) Neural networks: a comprehensive foundation. 2nd ed. Prentice Hall
39. Kingma DP, Ba J (2014) Adam: a Method for Stochastic Optimization. arXiv:1412.6980
40. Krogh A, Hertz JA (1991) A simple weight decay can improve generalization. Adv Neural Inform Proc Syst 4:950–957
41. Prechelt L (1998) Early stopping-but when? In: Neural Networks: Tricks of the trade. Springer, p. 55–69
42. Rasmussen C, Williams C (2006) Gaussian processes for machine learning. MIT Press
43. Head T, Kumar M, Nahrstaedt H, Louppe G, Shcherbatyi I (2020) Fu, editor.: scikit-optimize/scikit-optimize (v0.8.1). gitHub. https://doi.org/10.5281/zenodo.4014775
44. Pfeffer K, Bauer F, Morand L (2024) Temperature-dependent uniaxial stress relaxation dataset for C19010 copper alloy. Zenodo repository available at https://doi.org/10.5281/zenodo.10796926